Available online at www.sciencedirect.com
ScienceDirect
Journal of Computational Physics xxx (2008) xxx–xxx
JOURNAL OF COMPUTATIONAL PHYSICS
www.elsevier.com/locate/jcp

Boundary treatments in non-equilibrium Green's function (NEGF) methods for quantum transport in nano-MOSFETs

Haiyan Jiang [a], Sihong Shao [a], Wei Cai [b,*], Pingwen Zhang [a]

[a] *LMAM, CCSE and School of Mathematical Sciences, Peking University, Beijing 100871, China*
[b] *Department of Mathematics and Statistics, University of North Carolina at Charlotte, Charlotte, NC 28223, USA*

Received 8 November 2007; received in revised form 10 March 2008; accepted 16 March 2008

Abstract

Non-equilibrium Green's function (NEGF) is a general method for modeling non-equilibrium quantum transport in open mesoscopic systems with many body scattering effects. In this paper, we present a unified treatment of quantum device boundaries in the framework of NEGF with both finite difference and finite element discretizations. Boundary treatments for both types of numerical methods, and the resulting self-energy Σ for the NEGF formulism, representing the dissipative effects of device contacts on the transport, are derived using auxiliary Green's functions for the exterior of the quantum devices. Numerical results with both discretization schemes for an one-dimensional nano-device and a 29 nm double gated MOSFET are provided to demonstrate the accuracy and flexibility of the proposed boundary treatments.

Keywords: Non-equilibrium Green's function (NEGF); Self-energy; Quantum transport; Schrödinger equation; Nano-devices; MOSFET

1. Introduction

Numerical modeling of open quantum devices has become an indispensable tool to understand transport physics of devices scaled down to nano-meters. Non-equilibrium Green's function (NEGF) method is a comprehensive approach to address the quantum transport under biased external potential with many body and impurity scattering and device boundary effects [1–3]. In the limit of quasi-particle approximations (weak interaction between electrons and phonons and dilute impurities) and gradient approximations (slowly varying spatial and time external fields) [3], classical Boltzmann kinetic and drift diffusion formulations can be both derived from the NEGF. Electron density matrix and current can be expressed easily in terms of Green's functions in a simple form [2,4]. Using NEGF, ballistic transport and scattering transport have been studied in

* Corresponding author. Tel.: +1 704 687 4581; fax: +1 704 687 6415.
E-mail addresses: hyjiang@bit.edu.cn (H. Jiang), shaosihong@gmail.com (S. Shao), wcai@uncc.edu (W. Cai), pzhang@math.pku.edu.cn (P. Zhang).

0021-9991/$ - see front matter © 2008 Published by Elsevier Inc.
doi:10.1016/j.jcp.2008.03.018

[5]. The simulation tool nanoMOS [6] is a two-dimensional simulator using finite difference method (FDM) with NEGF. Mode-space method and real-space method are applied to double gate MOSFET simulation also within the NEGF framework [7].

As the quantum devices are usually integrated into a larger system, treatments for device boundaries are needed to limit the simulation size to reduce the cost of modeling using quantum mechanics. Therefore, it is of critical importance to pose boundary conditions at the boundaries between the contacts and the device. The effect of contacts on a device is usually described by a self-energy quantity Σ, which can be viewed as an effective potential or effective Hamiltonian. Self-energy can be derived by restricting the infinite domain Green's function into a finite region [2]. In fact, self-energy Σ is closely related to the artificial boundary conditions in the numerical solutions of NEGF [8,9]. For different numerical discretization of the Hamiltonian of the quantum device, such as FDM or finite element method (FEM), self-energy takes on different forms [10]. It is our objective in this paper to derive the explicit forms of the self-energies for both types of numerical discretizations in a unified manner.

In the numerical solutions of PDEs in a unbounded domain, artificial boundary conditions have been studied extensively in the application of FEM for stationary elliptic problems [11,12]. Also non-reflecting boundary conditions for time dependent Schrödinger equations have received much attentions for applications such as quantum physics [13,14], optic waveguide [15], and acoustics [16,17]. As those boundary conditions involve time convolution type integral operators at the boundaries, various fast algorithms have been proposed [13,18,19].

For electron transport in an open quantum system, traditional zero boundary condition and period boundary condition are not appropriate for describing non-equilibrium states under biased external voltage. To terminate the infinite exterior domain outside the device, several type of boundary treatments have been studied, including the popular quantum transmitting boundary method (QTBM) [20,21] and, the recent application of perfectly matched layer (PML) method [22]. In this paper, we will give a unified boundary treatment of open quantum devices appropriate for different numerical discretization techniques of NEGF for quantum transport. The QTBM will be a special case of our treatment for the finite element method of the NEGF. Exterior auxiliary Green's functions will be used to define the key quantity self-energy Σ, thus giving the proper boundary treatments in the NEGF formulation with both finite difference and finite element discretizations. The approach based on the exterior Green's functions allows boundary treatments for quantum devices of general shapes once the exterior Green's functions are obtained analytically or numerically [23], and yields boundary treatments suitable for FDM and FEM computations of NEGF.

The rest of the paper is organized as follows. In Section 2, we review some fundamental concepts of the NEGF formalism and introduce the self-consistent iteration of coupled NEGF and Poisson equation to address the space charge effects. The boundary treatments of NEGF with FDM and FEM discretizations, using auxiliary exterior Green's functions, are derived in Section 3 in one and two dimensions. The key step is the calculation of the self-energy Σ which embodies the influence of the exterior geometry of the quantum devices on the transport inside the devices. Finally, in Section 4, we will apply NEGF discretized by FDM and FEM equipped with the derived boundary treatments to simulate nano-devices, and analyze the performance of both methods. Section 5 contains the conclusions.

2. Non-equilibrium Green's function (NEGF) formalism and self-consistent solution

In the frame of NEGF, the Green's function for quantum transport in open systems is defined on the domain $\Omega = \Omega_D \cup \left(\sum_\alpha \Omega_\alpha\right)$ which consists of the device and contacts, $\Gamma = \partial\Omega$, see Fig. 1. Here Ω_D is the device region, Ω_α is the region of contact α which extends to infinity, $\Gamma_\alpha = \Gamma_D \cap \partial\Omega_\alpha$ with $\Gamma_D = \partial\Omega_D$. For a given energy E, the Green's function is defined by

$$(E - H)G(\boldsymbol{r}, \boldsymbol{r}') = \delta(\boldsymbol{r} - \boldsymbol{r}'), \quad \boldsymbol{r}, \boldsymbol{r}' \in \Omega, \tag{1}$$

where

$$H = -\frac{\hbar^2}{2}\nabla \cdot \left(\frac{1}{m(\boldsymbol{r})}\nabla\right) + V(\boldsymbol{r}) \tag{2}$$

Please cite this article in press as: H. Jiang et al., Boundary treatments in non-equilibrium Green's ..., J. Comput. Phys. (2008), doi:10.1016/j.jcp.2008.03.018

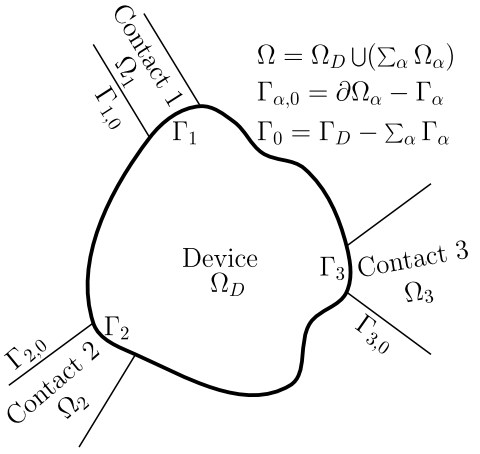

Fig. 1. Sketch of device and contacts. Ω_D is the device region enclosed by the bold curve, and Ω_α is the area of contact α with $\alpha = 1, 2, \ldots$. The boundary between Ω_D and Ω_α is denoted by Γ_α, while the rest of $\partial\Omega_\alpha$ is $\Gamma_{\alpha,0}$. $\Gamma_D = \partial\Omega_D$, and Ω is the whole region of the devices and the contacts.

is the Hamiltonian of the infinite system with an effective mass $m(\boldsymbol{r})$ and the Planck's constant $2\pi\hbar$, $V(\boldsymbol{r})$ is the potential energy. Here we assume that the Green's function $G(\boldsymbol{r}, \boldsymbol{r}')$ vanishes on the boundary Γ and satisfies Sommerfeld radiation conditions at infinite [23]. In practice, only Green's function of the device Ω_D is necessary, without the need for the details of the Green's functions in the remaining infinite exterior domain. To describe the coupling between the device and the contacts, a self-energy Σ quantity is introduced such that (1) is reformulated as

$$(E - H^0 - \Sigma)G(\boldsymbol{r}, \boldsymbol{r}') = \delta(\boldsymbol{r} - \boldsymbol{r}'), \quad \boldsymbol{r}, \boldsymbol{r}' \in \Omega_D, \tag{3}$$

where H^0 is the Hamiltonian of the isolated device region Ω_D, on which the actual computation will be done. The concept of self-energy Σ is far more general: $\Sigma = \sum_\alpha \Sigma^\alpha + \Sigma^s$ (in this paper, decoupling of the self-energies from different contacts and scattering events is assumed). And, the summation is with respect to all contacts, Σ^α accounts for the coupling between the device and contact α. The spatially distributed self-energy Σ^s describes the scattering inside the device (for example electrons–phonons or/and electrons–impurities) [1]. The correct modeling of the bodily self-energy Σ^s has to be done in the framework of second quantization to include many body scattering effects. The governing equation of the Green's function for the many body system will be either given by the Kadanoff–Baym differential equations or Dyson integral equations [3]. Despite of the complication from the modeling of the bodily self-energy Σ^s, the main differential equation for NEGF is basically of the form in Eq. (3). This is the reason why we focus our study of quantum transport in this work on Eq. (3), however, with the assumption $\Sigma^s = 0$, i.e., ballistic transport regime.

The Green's function and the self-energies are calculated with numerical methods for a given energy E. The resulting approximate solutions are then in a matrix form denoted by a mathematical boldface style, such as $\mathbf{G}(E)$ and $\mathbf{\Sigma}^\alpha(E)$. Since the discretization of $\delta(\boldsymbol{r} - \boldsymbol{r}')$ gives an identity matrix $\mathbf{I}$, we have

$$\mathbf{G}(E) = \left(\boldsymbol{\mathcal{E}}(E) - \mathbf{H}^0(E) - \sum_\alpha \mathbf{\Sigma}^\alpha(E) \right)^{-1}. \tag{4}$$

Denoting μ_α the Fermi level associated to contact α, the non-equilibrium density matrix is then given by [2]

$$\rho = \frac{1}{2\pi} \int_{-\infty}^{+\infty} \sum_\alpha f_{\mathrm{FD}}(E - \mu_\alpha) \mathbf{A}^\alpha(E) \, \mathrm{d}E, \tag{5}$$

where f_{FD} is the Fermi–Dirac distribution function

$$f_{\mathrm{FD}}(E - \mu_\alpha) = \left(1 + \exp\left(\frac{E - \mu_\alpha}{k_{\mathrm{B}} T} \right) \right)^{-1} \tag{6}$$

Please cite this article in press as: H. Jiang et al., Boundary treatments in non-equilibrium Green's ..., J. Comput. Phys. (2008), doi:10.1016/j.jcp.2008.03.018

with the Boltzmann constant k_B and the temperature T. And, the spectral function $\mathbf{A}^\alpha(E)$ is given as

$$\mathbf{A}^\alpha(E) = \mathbf{G}(E)\mathbf{\Gamma}^\alpha(E)\mathbf{G}^\dagger(E) \tag{7}$$

with a broadening function $\mathbf{\Gamma}^\alpha(E)$ reflecting the dissipative effects on the transport from contact α, defined by the imaginary part of the corresponding self-energy, i.e.

$$\mathbf{\Gamma}^\alpha(E) = \mathrm{i}(\mathbf{\Sigma}^\alpha(E) - (\mathbf{\Sigma}^\alpha(E))^\dagger). \tag{8}$$

The electron density $n(\boldsymbol{r})$ is given by the diagonal elements of the density matrix and depends on the potential $V(\boldsymbol{r})$ in the device. To account for the space charge effect, we have to use a self-consistent procedure with a Poisson equation for the potential. The potential distribution is then determined by coupling NEGF and the Poisson equation

$$-\nabla\cdot(\varepsilon(\boldsymbol{r})\nabla V(\boldsymbol{r})) = \mathrm{e}(-n(\boldsymbol{r}) + N_\mathrm{d}(\boldsymbol{r})), \tag{9}$$

where $N_\mathrm{d}(\boldsymbol{r})$ is the doping density, $\varepsilon(\boldsymbol{r})$ is the dielectric constant, and e is the electron charge. Appropriate boundary conditions for $V(\boldsymbol{r})$ will be specified in Section 4 for the simulated devices.

The self-consistent iteration solution is obtained as follows:

Step I: Start with an initial potential distribution $V(\boldsymbol{r}) = V_0$, let V_j be the resulting potential of the jth iteration, and we set to compute V_{j+1}.

Step II: For a given energy E, solve Green's function $\mathbf{G}(E)$ and self-energies $\mathbf{\Sigma}^\alpha(E)$ based on V_j, and then the spectral function $\mathbf{A}^\alpha(E)$.

Step III: Calculate the electron density $n(\boldsymbol{r})$ by integrating the density matrix ρ with respect to the energy E. It is noted that we need to repeat Step II for different sampling values of E for such an integration.

Step IV: Insert the electron density $n(\boldsymbol{r})$ into the Poisson equation (9), and obtain a new potential, namely, V_{j+1}.

Step V: Check $\|V_j - V_{j+1}\| < \epsilon$ (the given stop accuracy): if yes, stop; otherwise go to Step II.

Remark 1. In actual computation, there is no need to obtain the whole Green's function, only some blocks of the matrix $\mathbf{G}$ will be needed. This will be elaborated in Section 4.

Remark 2. Direct use of Eq. (9) leads to slow convergence. Instead, we will solve a nonlinear Poisson equation by a Newton's method [6].

Finally, the electron current between contacts 1 and 2, is given for a ballistic transport by [2]

$$I = \frac{\mathrm{e}}{\pi\hbar}\int_{-\infty}^{+\infty} T(E)(f_\mathrm{FD}(E-\mu_1) - f_\mathrm{FD}(E-\mu_2))\,\mathrm{d}E, \tag{10}$$

where $T(E)$ is the transmission coefficient defined by

$$T(E) = \mathrm{Trace}(\mathbf{\Gamma}^1(E)\mathbf{G}(E)\mathbf{\Gamma}^2(E)\mathbf{G}^\dagger(E)). \tag{11}$$

We can see that the most important quantities are the Green's function $\mathbf{G}(E)$ and the dissipative broadening function $\mathbf{\Gamma}^\alpha(E)$ (the imaginary part of the self-energy $\mathbf{\Sigma}^\alpha(E)$), from which we will be able to compute experimental observables such as current.

3. Computations with NEGF Methods and boundary treatments of open quantum devices

As we have seen in the last section, we need to evaluate G and Σ^α numerically. Different numerical discretization will give different forms for the Green's functions and the self-energies. Taking one-dimensional case as an example, FDM and FEM will be considered in a uniform mesh $\cdots < x_0 < x_1 < x_2 < \cdots < x_N < x_{N+1} < \cdots$ with a grid spacing a (see Fig. 2). We need to know the values of the Green's function $G(x,x')$ at the nodes $x_1 < x_2 < \cdots < x_N$ inside the device $\Omega_D = [x_1, x_N]$, which means we will solve Eq. (3) instead of Eq. (1). Denote

Please cite this article in press as: H. Jiang et al., Boundary treatments in non-equilibrium Green's ..., J. Comput. Phys. (2008), doi:10.1016/j.jcp.2008.03.018

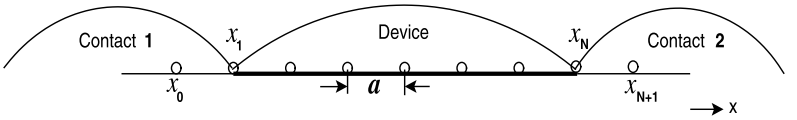

Fig. 2. One-dimensional discretization with a uniform mesh. a is the grid spacing. The computational domain Ω_D (the device area) is $[x_1, x_N]$. The unknowns are at the grid points x_i with $i = 1, \ldots, N$.

$\mathbf{G} = [G_{i,j}]_{N\times N} = [G(x_i, x_j)]_{N\times N}$ the matrix of the unknown nodal values of the Green's function corresponding to the given mesh.

- *NEGF with FDM* For illustration, we will use a second-order central difference scheme to solve Eq. (1) in Ω_D by using the following difference formulas

$$\frac{\partial}{\partial x}\left(\frac{1}{m}\frac{\partial u}{\partial x}\right)_{x=x_i} \approx \frac{1}{a^2}\left(\frac{u_{i+1}-u_i}{m_{i+1/2}} - \frac{u_i - u_{i-1}}{m_{i-1/2}}\right), \tag{12}$$

where $u_i = u(x_i)$ and $m_{i\pm1/2} = m\left(\frac{x_i + x_{i\pm1}}{2}\right)$, $i = 1, 2, \cdots, N$. When $i = 1$, the scheme becomes

$$\frac{\partial}{\partial x}\left(\frac{1}{m}\frac{\partial u}{\partial x}\right)_{x=x_1} \approx \frac{1}{a^2}\left(\frac{u_2-u_1}{m_{3/2}} - \frac{u_1 - u_0}{m_{1/2}}\right), \tag{13}$$

which means that we need to specify the nodal values $u_0 \equiv G_{0,j} = G(x_0, x_j)$ in terms of $G_{i,j} (i = 1, 2, \cdots, N)$ for any given $j \in \{1, 2, \cdots, N\}$. If a relation is given as

$$G_{0,j} = \sum_{i=1}^{N} \omega_i^1 G_{i,j}, \tag{14}$$

then, the self-energy $\mathbf{\Sigma}^1$ corresponding to the coupling between contact 1 and the device is

$$\Sigma^1_{p,q} = -\frac{\hbar^2}{2m_{1/2}a^2}\omega_q^1 \delta_{p,1}, \tag{15}$$

where $\delta_{i,j}$ is the Kroneckor notation. Similarly, the self-energy $\mathbf{\Sigma}^2$ coupling contact 2 and the device is

$$\Sigma^2_{p,q} = -\frac{\hbar^2}{2m_{N+1/2}a^2}\omega_q^2 \delta_{p,N}. \tag{16}$$

Meanwhile, the matrix $\mathbf{H}^0$ for the isolated device Hamiltonian H^0 is

$$\mathbf{H}^0 = \mathbf{V} + \frac{\hbar^2}{2a^2}\begin{bmatrix} -\frac{1}{m_{1/2}} - \frac{1}{m_{3/2}} & \frac{1}{m_{3/2}} & 0 & \cdots & \cdots & 0 \\ \frac{1}{m_{3/2}} & -\frac{1}{m_{3/2}} - \frac{1}{m_{5/2}} & \frac{1}{m_{5/2}} & \ddots & \ddots & \vdots \\ 0 & \frac{1}{m_{5/2}} & -\frac{1}{m_{5/2}} - \frac{1}{m_{7/2}} & \ddots & \ddots & \vdots \\ \vdots & \ddots & \ddots & \ddots & \ddots & 0 \\ \vdots & \ddots & \ddots & \ddots & -\frac{1}{m_{N-3/2}} - \frac{1}{m_{N-1/2}} & \frac{1}{m_{N-1/2}} \\ 0 & \cdots & \cdots & 0 & \frac{1}{m_{N-1/2}} & -\frac{1}{m_{N-1/2}} - \frac{1}{m_{N+1/2}} \end{bmatrix} \tag{17}$$

with $\mathbf{V} = \mathrm{diag}(V_1, V_2, \ldots, V_N)$.

Therefore, the device Green's function $\mathbf{G}(E)$ is given by Eq. (4) with Eqs. (15)–(17), $\boldsymbol{\mathcal{E}} = E\mathbf{I}$.

- *NEGF with FEM* Denoting $\varphi_i(x)$ as the shape function of FEM, we have

$$\varphi_i(x_j) = \delta_{i,j}, \tag{18}$$

and the approximation of the Green's function is then given as

$$G_h(x,x_j)=\sum_{i=1}^{N}G_{i,j}\varphi_i(x). \tag{19}$$

The weak form of Eq. (1) in Ω_D with a test function $\varphi(x)$ implies

$$E\int_{\Omega_D}G_h\varphi\,\mathrm{d}x-\frac{\hbar^2}{2}\int_{\Omega_D}\frac{1}{m}\frac{\partial G_h}{\partial x}\frac{\partial\varphi}{\partial x}\,\mathrm{d}x-\int_{\Omega_D}VG_h\varphi\,\mathrm{d}x-\frac{\hbar^2}{2}\left(\frac{1}{m}\frac{\partial G_h}{\partial x}\varphi\right)_{x=x_1}-\frac{\hbar^2}{2}\left(-\frac{1}{m}\frac{\partial G_h}{\partial x}\varphi\right)_{x=x_N}=\varphi(x_j), \tag{20}$$

where we have inserted the approximate function, and set the source $x'=x_j$. If the following relations hold

$$\frac{\partial G_h(x_1,x_j)}{\partial x}=\sum_{i=1}^{N}\varpi_i^1G_{i,j},\quad \frac{\partial G_h(x_N,x_j)}{\partial x}=\sum_{i=1}^{N}\varpi_i^2G_{i,j}, \tag{21}$$

then, the self-energies $\mathbf{\Sigma}^1$ and $\mathbf{\Sigma}^2$ will be just

$$\Sigma^1_{p,q}=\frac{\hbar^2}{2m_1}\varpi_q^1\delta_{p,1}, \tag{22}$$

$$\Sigma^2_{p,q}=-\frac{\hbar^2}{2m_N}\varpi_q^2\delta_{p,N}. \tag{23}$$

From the weak form (20), we also get the matrix form of H^0 as

$$H^0_{p,q}=\frac{\hbar^2}{2}\int_{\Omega_D}\frac{1}{m}\frac{\partial\varphi_q}{\partial x}\frac{\partial\varphi_p}{\partial x}\,\mathrm{d}x+\int_{\Omega_D}V\varphi_q\varphi_p\,\mathrm{d}x, \tag{24}$$

and

$$\boldsymbol{\mathcal{E}}=E\mathbf{S}\quad\text{with}\quad S_{p,q}=\int_{\Omega_D}\varphi_q\varphi_p\,\mathrm{d}x. \tag{25}$$

Again, the device Green's function $\mathbf{G}(E)$ in Eq. (4) is completely defined with Eqs. (22)–(25).

From the discussions above, we can see that the boundary relations (14) in FDM and (21) in FEM are necessary for evaluating the self-energies and the Green's functions. These relations actually are the boundary conditions for the numerical methods to be used. In the following, we will utilize the auxiliary Green's function $g(\boldsymbol{r},\boldsymbol{r}')$ to derive such boundary conditions for both FDM and FEM discretization of the NEGF in a unified treatment.

First, we will make the following assumption about the contacts.

Assumption 1. In the contact, the potential $V(\boldsymbol{r})$ is invariant by translation along the transport direction and the effective mass $m(\boldsymbol{r})$ is independent of position.

In order to find suitable boundary conditions for $G(\boldsymbol{r},\boldsymbol{r}')$ on Γ_α, an auxiliary Green's function $g(\boldsymbol{r},\boldsymbol{r}'_{\mathrm{e}})$ is defined by

$$(E-H)g(\boldsymbol{r},\boldsymbol{r}'_{\mathrm{e}})=\delta(\boldsymbol{r}-\boldsymbol{r}'_{\mathrm{e}}),\quad \boldsymbol{r},\boldsymbol{r}'_{\mathrm{e}}\in\Omega_\alpha, \tag{26}$$

which can be viewed as the restriction of Eq. (1) onto the semi-infinite region Ω_α plus a yet to be determined boundary condition on Γ_α. Here, the subscript 'e' denotes the exterior of the computational domain Ω_D.

Please cite this article in press as: H. Jiang et al., Boundary treatments in non-equilibrium Green's ..., J. Comput. Phys. (2008), doi:10.1016/j.jcp.2008.03.018

Subtracting the product of Eq. (1) and $g(\boldsymbol{r},\boldsymbol{r}'_e)$ from the product of Eq. (26) and $G(\boldsymbol{r},\boldsymbol{r}')$ with $\boldsymbol{r}'\in\Omega_D$, integrating with respect to $\boldsymbol{r}$ on Ω_α, and using the Green's formula, we have

$$\begin{aligned}G(\boldsymbol{r}'_e,\boldsymbol{r}') &= \int_{\Omega_\alpha} G(\boldsymbol{r},\boldsymbol{r}')\delta(\boldsymbol{r}-\boldsymbol{r}'_e)\,d\boldsymbol{r} - \int_{\Omega_\alpha} g(\boldsymbol{r},\boldsymbol{r}'_e)\delta(\boldsymbol{r}-\boldsymbol{r}')\,d\boldsymbol{r}\\ &= \int_{\Omega_\alpha}\frac{\hbar^2}{2m^\alpha}(\nabla^2 g(\boldsymbol{r},\boldsymbol{r}'_e)G(\boldsymbol{r},\boldsymbol{r}') - \nabla^2 G(\boldsymbol{r},\boldsymbol{r}')g(\boldsymbol{r},\boldsymbol{r}'_e))\,d\boldsymbol{r}\\ &= \int_{\partial\Omega_\alpha}\frac{\hbar^2}{2m^\alpha}\left(\frac{\partial g(\boldsymbol{r},\boldsymbol{r}'_e)}{\partial\boldsymbol{n}}G(\boldsymbol{r},\boldsymbol{r}') - \frac{\partial G(\boldsymbol{r},\boldsymbol{r}')}{\partial\boldsymbol{n}}g(\boldsymbol{r},\boldsymbol{r}'_e)\right)ds\\ &= \int_{\Gamma_\alpha}\frac{\hbar^2}{2m^\alpha}\left(\frac{\partial g(\boldsymbol{r},\boldsymbol{r}'_e)}{\partial\boldsymbol{n}}G(\boldsymbol{r},\boldsymbol{r}') - \frac{\partial G(\boldsymbol{r},\boldsymbol{r}')}{\partial\boldsymbol{n}}g(\boldsymbol{r},\boldsymbol{r}'_e)\right)ds,\end{aligned}\tag{27}$$

where m^α is the effective mass in contact α and $\boldsymbol{n}$ is the normal vector exterior to the boundary $\partial\Omega_\alpha$. Here we have used the fact that m_α is independent of position and both $G(\boldsymbol{r},\boldsymbol{r}')$ and $g(\boldsymbol{r},\boldsymbol{r}'_e)$ satisfy Sommerfeld radiation conditions at infinite and homogeneous Dirichlet conditions on $\Gamma_{\alpha,0}$.

According to Eq. (27), by assuming different boundary conditions for the auxiliary Green's function, we find

(1) If $g(\boldsymbol{r},\boldsymbol{r}'_e)=0$ for $\boldsymbol{r}\in\Gamma_\alpha$, i.e. homogeneous Dirichlet condition, then

$$G(\boldsymbol{r}'_e,\boldsymbol{r}') = \int_{\Gamma_\alpha}\frac{\hbar^2}{2m^\alpha}\frac{\partial g(\boldsymbol{r},\boldsymbol{r}'_e)}{\partial\boldsymbol{n}}G(\boldsymbol{r},\boldsymbol{r}')\,ds,\quad \boldsymbol{r}'_e\in\Omega_\alpha,\boldsymbol{r}'\in\Omega_D;\tag{28}$$

(2) If $\frac{\partial g(\boldsymbol{r},\boldsymbol{r}'_e)}{\partial\boldsymbol{n}}=0$ for $\boldsymbol{r}\in\Gamma_\alpha$, i.e. homogeneous Neumann condition, then

$$G(\boldsymbol{r}'_e,\boldsymbol{r}') = -\int_{\Gamma_\alpha}\frac{\hbar^2}{2m^\alpha}\frac{\partial G(\boldsymbol{r},\boldsymbol{r}')}{\partial\boldsymbol{n}}g(\boldsymbol{r},\boldsymbol{r}'_e)\,ds,\quad \boldsymbol{r}'_e\in\Omega_\alpha,\boldsymbol{r}'\in\Omega_D.\tag{29}$$

Noting that the Green's function satisfies the following continuity conditions [23] for $\boldsymbol{r}\in\Gamma_\alpha,\boldsymbol{r}'\in\Omega_D$,

$$\begin{cases} G(\boldsymbol{r}-,\boldsymbol{r}') = G(\boldsymbol{r}+,\boldsymbol{r}')\\ \frac{1}{m(\boldsymbol{r}-)}\frac{\partial G(\boldsymbol{r}-,\boldsymbol{r}')}{\partial\boldsymbol{n}} = \frac{1}{m(\boldsymbol{r}+)}\frac{\partial G(\boldsymbol{r}+,\boldsymbol{r}')}{\partial\boldsymbol{n}},\end{cases}\tag{30}$$

where $-$ $(+)$ denotes the limit from the exterior (interior) of Ω_D.

Remark 3. The continuity equation (30) needs some careful interpretation when both the source point $\boldsymbol{r}'$ and the field point $\boldsymbol{r}$ are on the device boundary Γ_α in deriving the device Green's function of Eq. (4). For this case, we will consider the source point $\boldsymbol{r}'$ by a limiting process from inside the device toward the device boundary, and in this way the continuity conditions (30) for the device Green's function can be used on the device boundary. This continuity is necessary to connect the values of the device Green's function from both sides of the device boundary, and obtain the self-energies Σ^α for the contacts in the rest of this paper.

Eqs. (28) and (29) yield boundary conditions for $G(\boldsymbol{r},\boldsymbol{r}')$ provided $g(\boldsymbol{r},\boldsymbol{r}'_e)$ is known. These boundary conditions will define the self-energy Σ^α corresponding to the contact Ω_α. Eq. (28) can be used in FDM to eliminate the unknowns at "ghost" points $\boldsymbol{r}'_e$ in Ω_α outside the computational domain Ω_D in terms of the solutions at the boundary points $\boldsymbol{r}$. Eq. (29) is the so-called Neumann-to-Dirichlet (NtD) mapping on Γ_α by letting $\boldsymbol{r}'_e\to\boldsymbol{r}_\alpha$ with $\boldsymbol{r}_\alpha\in\Gamma_\alpha$, and can be used in FEM to connect the solution and its normal derivative. In practice, it is more convenient to use a Dirichlet-to-Neumann (DtN) mapping which is the inverse of Eq. (29). We could get the DtN mapping as in [8] from Eq. (28). Differentiating Eq. (28) with respect to $\boldsymbol{r}'_e$, letting $\boldsymbol{r}'_e\to\boldsymbol{r}_\alpha$ and taking the normal derivative at $\boldsymbol{r}_\alpha$, we obtain

$$\frac{\partial G(\boldsymbol{r}_\alpha-,\boldsymbol{r}')}{\partial\boldsymbol{n}_\alpha} = \frac{\hbar^2}{2m^\alpha}\int_{\Gamma_\alpha}\frac{\partial^2 g(\boldsymbol{r},\boldsymbol{r}_\alpha-)}{\partial\boldsymbol{n}_\alpha\partial\boldsymbol{n}}G(\boldsymbol{r},\boldsymbol{r}')\,ds,\tag{31}$$

where $\boldsymbol{n}_\alpha$ denotes the outward normal of Ω_D at $\boldsymbol{r}_\alpha$.

Please cite this article in press as: H. Jiang et al., Boundary treatments in non-equilibrium Green's ..., J. Comput. Phys. (2008), doi:10.1016/j.jcp.2008.03.018

We will use Eqs. (28), (29) and (31) to derive the self-energies Σ^α for each contact and then calculate the Green's function in Eq. (4). To illustrate the idea, we use a strip shape contact although the method is for more general shape contact shown in Fig. 1. The analytical expressions for the auxiliary Green's function in a strip or a wedge shape can be found in the Appendix.

3.1. One-dimensional NEGF

For an ultra-small device with two large contacts (Fig. 2), the potential is given as

$$V(x) = \begin{cases} v^1 & -\infty < x < x_1 \\ v(x) & x_1 \leqslant x \leqslant x_N \\ v^2 & x_N < x < +\infty, \end{cases} \tag{32}$$

where v^α is the constant potential in contact $\alpha(\alpha = 1, 2)$. The corresponding Green's function is defined by

$$\left(E - V(x) + \frac{\hbar^2}{2}\frac{\partial}{\partial x}\left(\frac{1}{m}\frac{\partial}{\partial x}\right)\right) G(x, x') = \delta(x - x'), \quad x, x' \in (-\infty, +\infty). \tag{33}$$

As mentioned before, it is not necessary to compute the Green's function in the infinite domain but only the Green's function inside the device. However, boundary conditions at $x = x_1$ and $x = x_N$ are needed to compute G and $\Sigma^\alpha(\alpha = 1, 2)$, numerically. We will consider $x = x_1$, and the case of $x = x_N$ can be handled in a similar way. The auxiliary Green's function $g(x, x'_e)$ is defined in the domain $\Omega_1 = (-\infty, x_1)$ (the contact 1 area) as

$$\left(E - v^1 + \frac{\hbar^2}{2m^1}\frac{\partial^2}{\partial x^2}\right) g(x, x'_e) = \delta(x - x'_e), \quad x, x'_e \in \Omega_1. \tag{34}$$

- *Boundary treatment for NEGF with FDM*

Rewrite Eq. (28) as

$$G(x'_e, x') = \frac{\hbar^2}{2m^1}\frac{\partial g(x_1, x'_e)}{\partial x} G(x_1, x'), \tag{35}$$

which implies that

$$\omega_i^1 = \frac{\hbar^2}{2m^1}\frac{\partial g(x_1, x_0)}{\partial x}\delta_{i,1}. \tag{36}$$

From the analytical expression (A.3) in the Appendix for $g(x, x'_e)$ in a strip shape contact, we have

$$\omega_i^1 = \exp(\mathrm{i}k^1 a)\delta_{i,1}, \quad \omega_i^2 = \exp(\mathrm{i}k^2 a)\delta_{i,N}, \tag{37}$$

where $k^\alpha = \sqrt{\frac{2m^\alpha(E - v^\alpha)}{\hbar^2}}$ $(\alpha = 1, 2)$. According to Eqs. (15), (16) and (37), we obtain the self-energies

$$\Sigma^1_{p,q} = -\frac{\hbar^2}{2m^1 a^2}\exp(\mathrm{i}k^1 a)\delta_{q,1}\delta_{p,1}, \tag{38}$$

$$\Sigma^2_{p,q} = -\frac{\hbar^2}{2m^2 a^2}\exp(\mathrm{i}k^2 a)\delta_{q,N}\delta_{p,N}, \tag{39}$$

which agree with those given in [2].

- *Boundary treatment for NEGF with FEM*

Rewriting Eq. (29), we have

$$G(x'_e, x') = -\frac{\hbar^2}{2m^1}\frac{\partial G(x_1, x')}{\partial x} g(x_1, x'_e). \tag{40}$$

Please cite this article in press as: H. Jiang et al., Boundary treatments in non-equilibrium Green's ..., J. Comput. Phys. (2008), doi:10.1016/j.jcp.2008.03.018

Letting $x'_e \to x_1$ and noting Eq. (30), it becomes

$$G(x_1,x') = -\frac{\hbar^2}{2m^1}\frac{\partial G(x_1-,x')}{\partial x}g(x_1,x_1-) = -\frac{\hbar^2}{2m^1}\frac{m^1}{m_1}\frac{\partial G(x_1+,x')}{\partial x}g(x_1,x_1-), \tag{41}$$

where m^1 is the constant effective mass in contact 1 and $m_1 = m(x_1)$. Using the analytical expression (A.4) of $g(x,x'_e)$ in the Appendix, we can get

$$\varpi_i^1 = -\mathrm{i}k^1\frac{m_1}{m^1}\delta_{i,1}, \tag{42}$$

from which, the self-energy $\mathbf{\Sigma}^1$ for contact 1 is

$$\Sigma^1_{p,q} = -\frac{\hbar^2}{2m^1}\mathrm{i}k^1\delta_{q,1}\delta_{p,1}. \tag{43}$$

Similarly, we can find the self-energy $\mathbf{\Sigma}^2$ for contact 2 as

$$\Sigma^2_{p,q} = -\frac{\hbar^2}{2m^2}\mathrm{i}k^2\delta_{q,N}\delta_{p,N}. \tag{44}$$

3.2. Two-dimensional NEGF

If a two-dimensional quantum device is wide in y-direction, we can assume that $G(\boldsymbol{r},\boldsymbol{r}')$ is independent of y, i.e. a function of (x,z) only. We consider the ultra-small MOSFET simulation in the strip region Ω (see Fig. 3), which consists of three sub-domains: the contact 1 area Ω_1, the device area Ω_D, and the contact 2 area Ω_2. The following notations and specifications will be used for the two-dimensional problem,

$$\Omega = \Omega_1 \cup \Omega_D \cup \Omega_2$$
$$\Omega_1 = \{(x,z)|x \in (-\infty, x_1), z \in [0,L]\}$$
$$\Omega_D = \{(x,z)|x \in [x_1, x_{N_x}], z \in [0,L]\}$$
$$\Omega_2 = \{(x,z)|x \in (x_{N_x}, +\infty), z \in [0,L]\}$$
$$\Gamma_1 = \partial\Omega_1 \cap \partial\Omega_D = \{(x,z)|x = x_1, z \in [0,L]\}$$
$$\Gamma_2 = \partial\Omega_2 \cap \partial\Omega_D = \{(x,z)|x = x_{N_x}, z \in [0,L]\}$$
$$\Gamma_t = \{(x,z)|x \in [-\infty,+\infty], z = L\}$$
$$\Gamma_b = \{(x,z)|| \in [-\infty,+\infty], z = 0\}$$

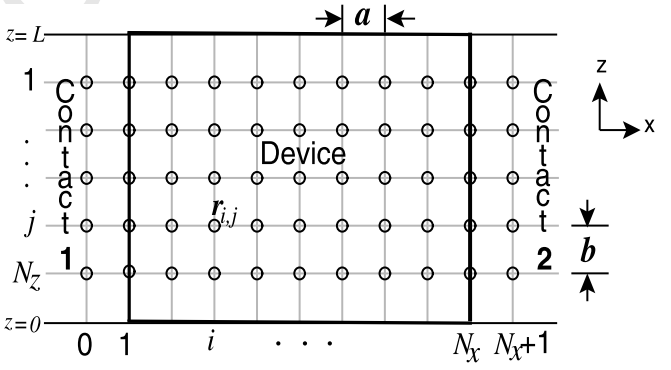

Fig. 3. Two-dimensional discretization with a uniform mesh (the gray lines). a is the grid spacing in x-direction, while b for y-direction. The computational domain Ω_D is the central area surrounded by the bold black lines. The width in z-direction is L. The homogeneous Dirichlet conditions on the top and bottom boundaries are used. The unknowns are at the grid points $\boldsymbol{r}_q = \boldsymbol{r}_{i,j} = (x_i, z_j)$ with $q = (i-1)N_z + j, i = 1,\ldots,N_x$, $j = 1,\ldots,N_z$, and $q = 1,2,\ldots,N$. $N = N_xN_z$ is the number of unknowns. We can see here the order of unknowns is z-direction first.

Please cite this article in press as: H. Jiang et al., Boundary treatments in non-equilibrium Green's ..., J. Comput. Phys. (2008), doi:10.1016/j.jcp.2008.03.018

As in the one-dimensional case, the computational domain is denoted as Ω_D. Let L be the thickness of the silicon layer, or the combined thickness of the silicon layer and the oxide layer if tunneling effects are to be included. When electron tunneling into the oxide regions is neglected, the homogeneous Dirichlet conditions can be used on the top and bottom boundaries. Assumption 1 for the contact means that the band structure is independent of x in the contact area, thus, we have

$$V(\boldsymbol{r}) = \begin{cases} v^1(z) & \boldsymbol{r} \in \Omega_1 \\ v(x,z) & \boldsymbol{r} \in \Omega_D \\ v^2(z) & \boldsymbol{r} \in \Omega_2, \end{cases} \tag{45}$$

where $\boldsymbol{r} = (x,z) \in \Omega$. The relevant Green's function is defined by

$$\left(E - V(\boldsymbol{r}) + \frac{\hbar^2}{2}\nabla \cdot \left(\frac{1}{m}\nabla\right)\right) G(\boldsymbol{r},\boldsymbol{r}') = \delta(\boldsymbol{r}-\boldsymbol{r}'), \quad \boldsymbol{r},\boldsymbol{r}' \in \Omega, \tag{46}$$

where $\nabla = (\frac{\partial}{\partial x}, \frac{\partial}{\partial z})$. In order to get a finite discrete system, we need to give suitable boundary conditions on Γ_α, to obtain the self-energies $\Sigma^\alpha (\alpha = 1,2)$ as in the one-dimensional case. Let us only deal with Γ_1 as an example, i.e., the computation of Σ^1. The calculation of Σ^2 is similar. Again, we define an auxiliary Green's function $g(\boldsymbol{r},\boldsymbol{r}'_e)$, which satisfies in Ω_1

$$\left(E - v^1(z) + \frac{\hbar^2}{2m^1}\nabla^2\right) g(\boldsymbol{r},\boldsymbol{r}'_e) = \delta(\boldsymbol{r}-\boldsymbol{r}'_e), \quad \boldsymbol{r},\boldsymbol{r}'_e \in \Omega_1. \tag{47}$$

We will compute the self-energy Σ^1 and the Green's function G with both FDM and FEM. The unknowns are at the nodes $\boldsymbol{r}_q = \boldsymbol{r}_{i,j}$ (see Fig. 3). For a given source $\boldsymbol{r}' = \boldsymbol{r}_{q'} = \boldsymbol{r}_{i',j'}$, denoting $G_{q,q'} = G(\boldsymbol{r}_q, \boldsymbol{r}_{q'})$ and $\mathbf{G} = [G_{q,q'}]_{N\times N}$, the unknown vector is the q'th column of $\mathbf{G}$, with $N = N_x N_z$ the number of unknowns. We need to solve one matrix system for each given source location. The notations $G_{i,j,i',j'}$, $G_{i,j,q'}$, and $G_{q,q'}$ will be used, interchangeably.

- *NEGF with FDM* While using the second-order central difference scheme, we need boundary conditions when computing the unknowns at Γ_1. To compute $G_{1,j,q'}$ (q' is fixed), we should express $G_{0,j,q'}$ using $G_{q,q'}, q = 1,\ldots,N$, $j = 1,\ldots,N_z$. Suppose that we have a relationship as follows

$$G_{0,j,q'} = \sum_{q=1}^{N} \omega_q^{1,j} G_{q,q'}, \tag{48}$$

and, then

$$\Sigma^1_{p,q} = \begin{cases} -\frac{\hbar^2}{2m_{1/2,p}a^2}\omega_q^{1,p}, & \text{if } p \in \{1,\ldots,N_z\} \\ 0, & \text{otherwise,} \end{cases} \tag{49}$$

where $m_{1/2,p} = m(\frac{x_0+x_1}{2}, z_p)$.

- *NEGF with FEM* The shape function $\varphi_q(\boldsymbol{r})$, corresponding to the node $\boldsymbol{r}_q$, satisfies

$$\varphi_q(\boldsymbol{r}_{q'}) = \delta_{q,q'}. \tag{50}$$

The approximate solution, for a given source point $\boldsymbol{r}_{q'}$, can be written as

$$G_h(\boldsymbol{r},\boldsymbol{r}_{q'}) = \sum_{q=1}^{N} G_{q,q'}\varphi_q(\boldsymbol{r}). \tag{51}$$

The weak form of Eq. (46) in the computational domain Ω_D for any test function $\varphi(\boldsymbol{r})$ is then

$$E\int_{\Omega_D} G_h\varphi\,\mathrm{d}\boldsymbol{r} - \int_{\Omega_D} VG_h\varphi\,\mathrm{d}\boldsymbol{r} - \frac{\hbar^2}{2}\int_{\Omega_D}\frac{1}{m}\nabla G_h\cdot\nabla\varphi\,\mathrm{d}\boldsymbol{r} + \frac{\hbar^2}{2}\int_{\Gamma_D}\frac{1}{m}\frac{\partial G_h}{\partial \boldsymbol{n}}\varphi\,\mathrm{d}s = \varphi(\boldsymbol{r}_{q'}), \tag{52}$$

Please cite this article in press as: H. Jiang et al., Boundary treatments in non-equilibrium Green's ..., J. Comput. Phys. (2008), doi:10.1016/j.jcp.2008.03.018

where G_h is the approximate solution, $\boldsymbol{n}$ is the outward unit normal of Ω_D, and the source is located at $\boldsymbol{r}_{q'}$. Noting that Ω_D is the rectangle region shown in Fig. 3, the surface integral in Eq. (52) can be rewritten as

$$\frac{\hbar^2}{2}\int_0^L \left(\frac{1}{m}\frac{\partial G_h}{\partial x}\varphi\right)\Big|_{x=x_1}^{x=x_{N_x}} \mathrm{d}z + \frac{\hbar^2}{2}\int_{x_1}^{x_{N_x}} \left(\frac{1}{m}\frac{\partial G_h}{\partial z}\varphi\right)\Big|_{z=0}^{z=L} \mathrm{d}x. \tag{53}$$

The second integral in Eq. (53) is zero due to the homogeneous Dirichlet conditions on Γ_t and Γ_b, while the first one reads

$$-\frac{\hbar^2}{2}\int_0^L \frac{1}{m(x_1,z)}\frac{\partial G_h(x_1,z,\boldsymbol{r}_{q'})}{\partial x}\varphi(x_1,z)\,\mathrm{d}z + \frac{\hbar^2}{2}\int_0^L \frac{1}{m(x_{N_x},z)}\frac{\partial G_h(x_{N_x},z,\boldsymbol{r}_{q'})}{\partial x}\varphi(x_{N_x},z)\,\mathrm{d}z. \tag{54}$$

We will identify the self-energies with the above surface integrals. To compute $\Sigma^1(\Sigma^2)$, we consider the first (second) integral in (54). If we have a relation in the form of

$$\frac{\partial G_h(x_1,z,\boldsymbol{r}_{q'})}{\partial x} = \widehat{\Sigma}^1 \cdot G_h(x_1,\tilde{z},\boldsymbol{r}_{q'}), \tag{55}$$

namely, the operator $\widehat{\Sigma}^1$ is exactly the DtN mapping on $\tilde{z}\in\Gamma_1$. Then, we can rewrite the first integral in (54) as

$$\begin{aligned}\frac{\hbar^2}{2}\int_0^L \frac{1}{m(x_1,z)}\frac{\partial G_h(x_1,z,\boldsymbol{r}_{q'})}{\partial x}\varphi(x_1,z)\,\mathrm{d}z &= \frac{\hbar^2}{2}\int_0^L \frac{1}{m(x_1,z)}(\widehat{\Sigma}^1\cdot G_h(x_1,\tilde{z},\boldsymbol{r}_{q'}))\varphi(x_1,z)\,\mathrm{d}z\\ &= \frac{\hbar^2}{2}\int_0^L \frac{1}{m(x_1,z)}\left(\hat{\Sigma}^1\cdot\left(\sum_{q=1}^N G_{q,q'}\varphi_q(x_1,\tilde{z})\right)\right)\varphi(x_1,z)\,\mathrm{d}z\\ &= \sum_{q=1}^N G_{q,q'}\frac{\hbar^2}{2}\int_0^L \frac{1}{m(x_1,z)}(\widehat{\Sigma}^1\cdot\varphi_q(x_1,\tilde{z}))\varphi(x_1,z)\,\mathrm{d}z,\end{aligned} \tag{56}$$

from which, we can define the self-energy $\boldsymbol{\Sigma}^1$ as

$$\Sigma^1_{p,q} = \frac{\hbar^2}{2}\int_0^L \frac{1}{m(x_1,z)}(\widehat{\Sigma}^1\cdot\varphi_q(x_1,\tilde{z}))\varphi_p(x_1,z)\,\mathrm{d}z. \tag{57}$$

- *Boundary treatment for NEGF with FDM*

Inserting the analytical expression of $g(\boldsymbol{r},\boldsymbol{r}'_{\mathrm{e}})$ of Eq. (A.8) in the Appendix into Eq. (28), we obtain,

$$G(x'_{\mathrm{e}},z'_{\mathrm{e}},x',z') = \int_0^L G(x_1,z,x',z')\sum_l \chi^1_l(z)\chi^1_l(z'_{\mathrm{e}})\exp(-\mathrm{i}k^1_l(x'_{\mathrm{e}}-x_1))\,\mathrm{d}z \tag{58}$$

with $\chi^\alpha_l(z)$ and k^α_l defined in the Appendix. From Eq. (58) with a N_z-point trapezoid rule for the integration along Γ_1, we have

$$\begin{aligned}G(x_0,z_j,x',z') &= \sum_l \int_0^L G(x_1,z,x',z')\chi^1_l(z)\chi^1_l(z_j)\exp(\mathrm{i}k^1_l a)\,\mathrm{d}z\\ &\approx \sum_l\sum_{\tilde{j}=1}^{N_z} bG(x_1,z_{\tilde{j}},x',z')\chi^1_l(z_{\tilde{j}})\chi^1_l(z_j)\exp(\mathrm{i}k^1_l a)\\ &= \sum_{\tilde{j}=1}^{N_z}\sum_l bG(x_1,z_{\tilde{j}},x',z')\chi^1_l(z_{\tilde{j}})\chi^1_l(z_j)\exp(\mathrm{i}k^1_l a),\end{aligned} \tag{59}$$

from which we can see that

$$\omega^{1,j}_q = \begin{cases}\sum_l b\chi^1_l(z_q)\chi^1_l(z_j)\exp(\mathrm{i}k^1_l a) & \text{if } q\in\{1,\ldots,N_z\}\\ 0 & \text{otherwise.}\end{cases} \tag{60}$$

Therefore, the self-energy $\mathbf{\Sigma}^1$ for the NEGF with FDM is

$$\Sigma^1_{p,q} = \begin{cases} -\frac{\hbar^2}{2m^1a^2}\sum_l b\chi^1_l(z_q)\chi^1_l(z_p)\exp(\mathrm{i}k^1_l a), & \text{if } p,q \in \{1,\ldots,N_z\} \\ 0, & \text{otherwise.} \end{cases} \tag{61}$$

Truncating the infinite series to a finite order M, we get the self-energy as

$$\mathbf{\Sigma}^1 = \mathbf{Q}\mathbf{\Lambda}\mathbf{Q}^{\mathrm{T}}, \tag{62}$$

where

$$\mathbf{Q} = \begin{bmatrix} \chi^1_1(z_1) & \chi^1_2(z_1) & \cdots & \chi^1_M(z_1) \\ \chi^1_1(z_2) & \chi^1_2(z_2) & \cdots & \chi^1_M(z_2) \\ \vdots & \vdots & \vdots & \vdots \\ \chi^1_1(z_{N_z}) & \chi^1_2(z_{N_z}) & \cdots & \chi^1_M(z_{N_z}) \\ 0 & 0 & \cdots & 0 \\ \vdots & \vdots & \vdots & \vdots \\ 0 & 0 & \cdots & 0 \end{bmatrix}_{N\times M} \tag{63}$$

and

$$\mathbf{\Lambda} = -\frac{\hbar^2 b}{2m^1a^2}\mathrm{diag}(\exp(\mathrm{i}k^1_1 a), \exp(\mathrm{i}k^1_2 a), \ldots, \exp(\mathrm{i}k^1_M a))_{M\times M}. \tag{64}$$

- *Boundary treatment for NEGF with FEM*

Using the analytical expression of $g(\boldsymbol{r}, \boldsymbol{r}'_{\mathrm{e}})$ from Eq. (A.8) in the Appendix into Eq. (31), we have

$$\frac{\partial G(x_1-, z'_{\mathrm{e}}, x', z')}{\partial x} = \int_0^L G(x_1, z, x', z')\sum_l \chi^1_l(z)\chi^1_l(z'_{\mathrm{e}})(-\mathrm{i}k^1_l)\,\mathrm{d}z. \tag{65}$$

According to Eqs. (30) and (55), we arrive

$$\widehat{\Sigma}^1 \cdot \varphi_q(x_1, \tilde{z}) = \frac{m(x_1,z)}{m^1}\int_0^L \varphi_q(x_1,\tilde{z})\sum_l \chi^1_l(\tilde{z})\chi^1_l(z)(-\mathrm{i}k^1_l)\,\mathrm{d}\tilde{z}, \tag{66}$$

and then, the self-energy $\mathbf{\Sigma}^1$ for the NEGF with FEM is

$$\begin{aligned} \Sigma^1_{p,q} &= \frac{\hbar^2}{2}\int_0^L \frac{1}{m(x_1,z)}\left(\frac{m(x_1,z)}{m^1}\int_0^L \varphi_q(x_1,\tilde{z})\sum_l \chi^1_l(\tilde{z})\chi^1_l(z)(-\mathrm{i}k^1_l)\,\mathrm{d}\tilde{z}\right)\varphi_p(x_1,z)\,\mathrm{d}z \\ &= \frac{\hbar^2}{2}\sum_l \frac{-\mathrm{i}k^1_l}{m^1}\left(\int_0^L \chi^1_l(z)\varphi_p(x_1,z)\,\mathrm{d}z\right)\left(\int_0^L \chi^1_l(\tilde{z})\varphi_q(x_1,\tilde{z})\,\mathrm{d}\tilde{z}\right). \end{aligned} \tag{67}$$

Truncating the infinite series to a finite order M, we have the self-energy with FEM in the same matrix form as Eq. (62). However, different expressions for $\mathbf{Q} = (Q_{p,l})_{N\times M}$ and $\mathbf{\Lambda}$ are given as follows,

$$Q_{p,l} = \int_0^L \chi^1_l(z)\varphi_p(x_1,z)\,\mathrm{d}z, \tag{68}$$

and

$$\mathbf{\Lambda} = -\frac{\mathrm{i}\hbar^2}{2m^1}\mathrm{diag}\left(k^1_1, k^1_2, \ldots, k^1_M\right)_{M\times M.} \tag{69}$$

Please cite this article in press as: H. Jiang et al., Boundary treatments in non-equilibrium Green's ..., J. Comput. Phys. (2008), doi:10.1016/j.jcp.2008.03.018

Remark 4. According to Eqs. (8) and (62), and using the fact that matrix $\mathbf{Q}$ is real, we can show that

$$\mathbf{\Gamma}^1 = \mathbf{Q}\mathbf{\Xi}\mathbf{Q}^{\mathrm{T}}, \tag{70}$$

where

$$\mathbf{\Xi} = \mathrm{i}(\mathbf{\Lambda} - \mathbf{\Lambda}^{\dagger}). \tag{71}$$

Using Eqs. (64) or (69), we get the following decomposition

$$\mathbf{\Gamma}^1 = \mathbf{\Upsilon}^{+}(\mathbf{\Upsilon}^{+})^{\dagger} - \mathbf{\Upsilon}^{-}(\mathbf{\Upsilon}^{-})^{\dagger}. \tag{72}$$

For example, using (69), we rewrite Eq. (71) as

$$\mathbf{\Xi} = \frac{\hbar^2}{m^1}\mathrm{diag}(Re(k_1^1), Re(k_2^1), \ldots, Re(k_M^1)), \tag{73}$$

where $Re(x)$ denotes the real part of x. Let $\mathbf{\Xi}^{+} = (\Xi^{+}_{i,j})_{M\times M}$ and $\mathbf{\Xi}^{-} = (\Xi^{-}_{i,j})_{M\times M}$ with

$$\Xi^{+}_{i,j} = \begin{cases} \Xi_{i,j} & \text{if } \Xi_{i,j} \geqslant 0 \\ 0 & \text{otherwise} \end{cases} \quad \text{and} \quad \Xi^{-}_{i,j} = \begin{cases} 0 & \text{if } \Xi_{i,j} \geqslant 0 \\ -\Xi_{i,j} & \text{otherwise,} \end{cases} \tag{74}$$

we have $\mathbf{\Xi} = \mathbf{\Xi}^{+} - \mathbf{\Xi}^{-}$, and then

$$\mathbf{\Gamma}^1 = \mathbf{Q}\sqrt{\mathbf{\Xi}^{+}}\sqrt{\mathbf{\Xi}^{+}}\mathbf{Q}^{\mathrm{T}} - \mathbf{Q}\sqrt{\mathbf{\Xi}^{-}}\sqrt{\mathbf{\Xi}^{-}}\mathbf{Q}^{\mathrm{T}}, \tag{75}$$

i.e. $\mathbf{\Upsilon}^{\pm} = \mathbf{Q}\sqrt{\mathbf{\Xi}^{\pm}}$.

4. Simulation of one- and two-dimensional devices

The NEGF calculated in Section 3, will be coupled with a Poisson equation solved for a self-consistent solution in this section. Both FDM and FEM are applied to one- and two-dimensional coupled Poisson equation and NEGF. The meshes are shown in Figs. 2 and 3, respectively. The second-order central difference scheme and $\mathcal{P}^1$ finite element [8] will be used in FDM and FEM, respectively.

We need to compute the spectral function $\mathbf{A}^{\alpha}(E)$ which is expressed in terms of the Green's function $\mathbf{G}(E)$ and the broadening function $\mathbf{\Gamma}^{\alpha}(E)$ in Eq. (7). After computing self-energies in Section 3, we can easily get the broadening function by Eq. (8). However, we only need to calculate part of the Green's function matrix. Take $\mathbf{A}^1(E)$ as an example.

- In one dimensional cases, noting that $\mathbf{\Gamma}^1$ is zero except $\Gamma^1_{1,1} \neq 0$, therefore only the first column of $\mathbf{G}$ will be used in calculating $\mathbf{A}^1$.
- In two dimensional cases, from the Remark 4 in Section 3, we know the decomposition $\mathbf{\Gamma}^1 = \mathbf{\Upsilon}\mathbf{\Upsilon}^{\dagger}$ (suppose here $\mathbf{\Xi}$ is non-negative for simplicity, i.e. $\mathbf{\Upsilon} = \mathbf{\Upsilon}^{+}$, for general case just repeat once for $\mathbf{\Upsilon} = \mathbf{\Upsilon}^{-}$ as in Eq. (72)), and then $\mathbf{A}^1 = \mathbf{G}\mathbf{\Upsilon}\mathbf{\Upsilon}^{\dagger}\mathbf{G}^{\dagger} = \mathbf{Y}\mathbf{Y}^{\dagger}$ with $\mathbf{Y} = \mathbf{G}\mathbf{\Upsilon}$ which means that

$$(\mathbf{E} - \mathbf{H}^0 - \sum_{\alpha}\mathbf{\Sigma}^{\alpha})\mathbf{Y} = \mathbf{\Upsilon}. \tag{76}$$

The column number of $\mathbf{\Upsilon}$ is the truncation order M in z-direction. Only a few lowest sub-energy bands are important, so only a few columns of $\mathbf{\Upsilon}$ are needed to obtain $\mathbf{A}^1$ by solving Eq. (76), instead of calculating the whole Green's function matrix $\mathbf{G}$.

Due to the jump discontinuity of the doping function, the accuracy of regular central finite difference scheme will degenerate at the interface between the high doping area and the low doping one. To improve the precision, we smooth the doping function at the interface with a linear interpolation. The numerical results show the effectiveness of this technique. The error at the interface of the doping function is less than elsewhere.

Please cite this article in press as: H. Jiang et al., Boundary treatments in non-equilibrium Green's ..., J. Comput. Phys. (2008), doi:10.1016/j.jcp.2008.03.018

4.1. One-dimensional device

Noting the space charge neutrality at the source (drain), the homogeneous Neumann boundary condition will be used at $x = x_1 (x = x_N)$ for the Poisson equation.

We consider the $n^{++} - n^{+} - n^{++}$ device (Fig. 4) used in [4]. The parameters are: $m = 0.25 m_0, m_0 = 9.1 \times 10^{31}$ kg, $\varepsilon = 10\varepsilon_0$, $\varepsilon_0 = 8.85 \times 10^{12}$ Fm^{-1}, $N_d = 10^{20}$ cm^{-3} in the n^{++} regions, each of which is 4.5 nm long, and $N_d = 5 \times 10^{19}$ cm^{-3} in the 21 nm n^{+} region.

Let the bias be $V_{ds} = 0.25$ V. Fig. 5 is the density function of electron, and Fig. 6 is the potential distribution with both FDM and FEM. We can see here that the density and potential functions show no difference of performance for FDM and FEM. To analyze these two methods further, numerical solution with fine enough mesh, for example $N = 1600$, is taken as a reference solution. For simplicity, equilibrium state i.e. the bias $V_{ds} = 0.0$ V is considered. Fig. 7 is the potential distribution at equilibrium. As the mesh is refined, the potential error decreases. Figs. 8 and 9 indicate that the two numerical methods are convergent. Fig. 10 shows that the FEM is more accurate than FDM, especially at the boundaries as expected.

To compute the convergence order numerically, let E_a be the L^2 error corresponding to the cell size a. The numerical convergence order is defined as $\log_2\left(\frac{E_a}{E_{a/2}}\right)$. Table 2 lists the numerical convergence order of the two numerical methods at the second order.

4.2. A 29 nm double gate MOSFET

The geometry of a double gate MOSFET is shown in Fig. 11 [6]. The width of the device is assumed to be large, and the potential is invariant along y-direction. The silicon layer is sandwiched by two symmetric oxide layers. Source and drain are doped heavily.

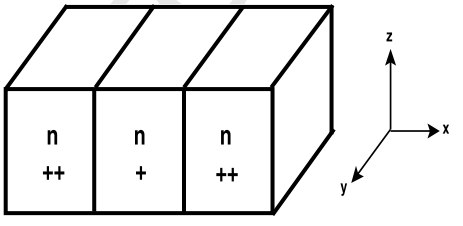

Fig. 4. A one-dimensional device in [4]. We only consider the transport in x-direction.

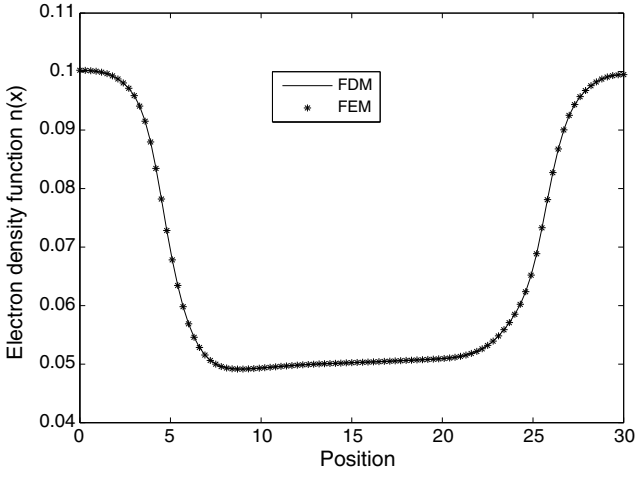

Fig. 5. One-dimensional device: the density function at bias $V_{ds} = 0.25$ V.

Please cite this article in press as: H. Jiang et al., Boundary treatments in non-equilibrium Green's ..., J. Comput. Phys. (2008), doi:10.1016/j.jcp.2008.03.018

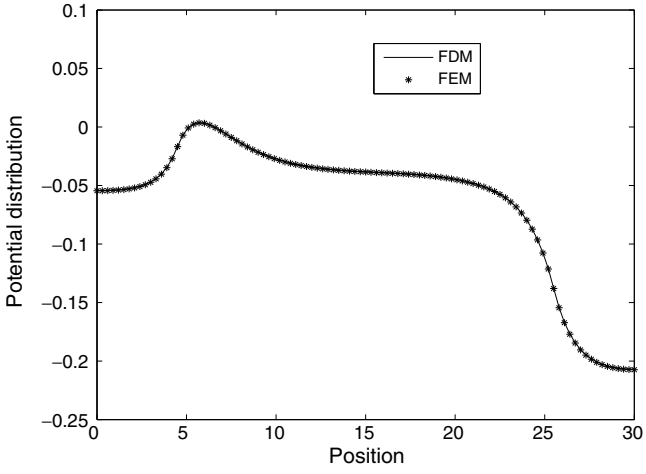

Fig. 6. One-dimensional device: the potential distribution at bias $V_{ds} = 0.25$ V.

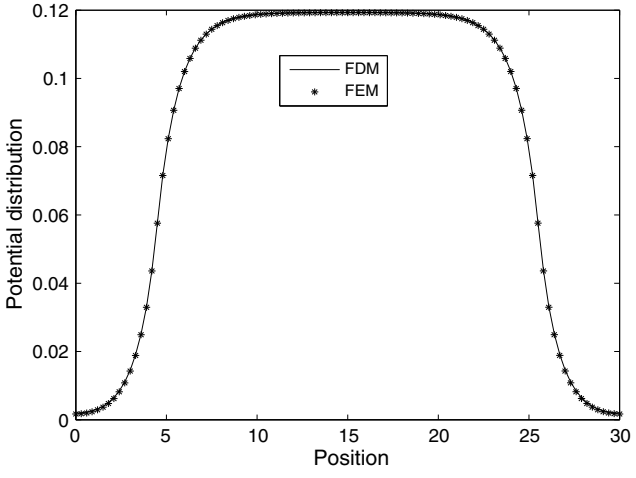

Fig. 7. One-dimensional device: the potential distribution at bias $V_{ds} = 0$ V.

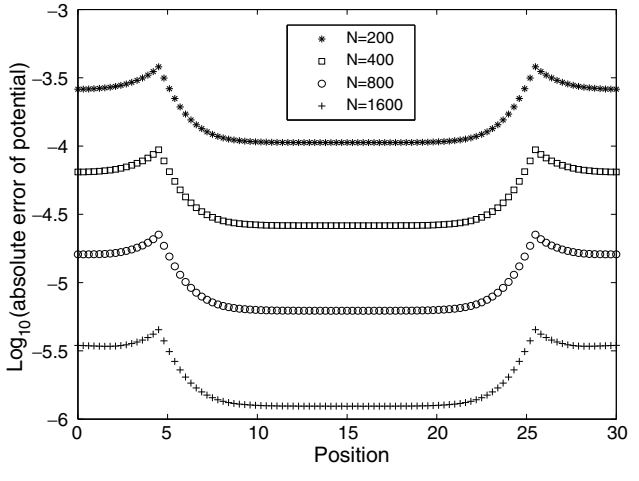

Fig. 8. One-dimensional device: the convergence history of FDM.

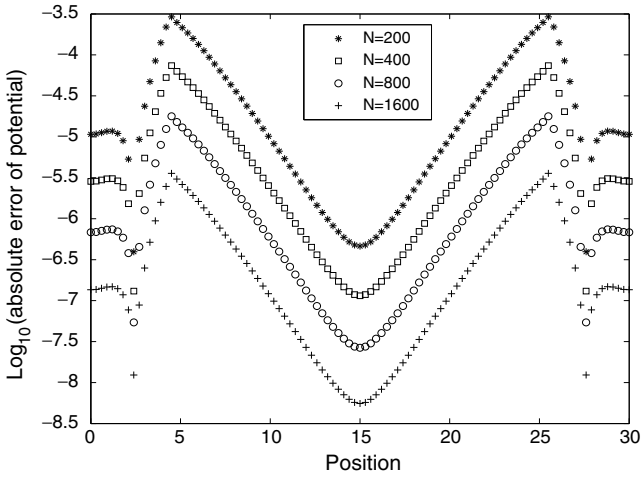

Fig. 9. One-dimensional device: the convergence history of FEM.

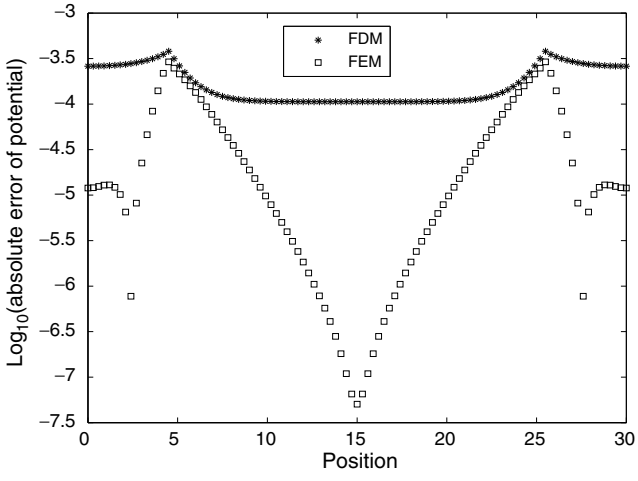

Fig. 10. One-dimensional device: comparison between FDM and FEM.

Table 1
Double gate MOSFET: numerical convergence order for two-dimensional case

Method	Convergence order
FDM	1.9018
FEM	1.9072

Table 2
One-dimensional device: numerical convergence order for one-dimensional case

	$N = 100$	$N = 200$	$N = 400$	$N = 800$
FDM	3.3091	2.0174	2.0527	2.2939
FEM	1.9670	2.0013	2.0651	2.3193

Please cite this article in press as: H. Jiang et al., Boundary treatments in non-equilibrium Green's ..., J. Comput. Phys. (2008), doi:10.1016/j.jcp.2008.03.018

The Poisson equation is solved in the rectangle region ABCD including the silicon layer and the oxide layer with the boundary condition

$$\begin{cases} V(\boldsymbol{r}) = V_g & \boldsymbol{r} \in \mathrm{EF},\ \mathrm{GH} \\ \frac{\partial V(\boldsymbol{r})}{\partial \boldsymbol{n}} = 0 & \boldsymbol{r} \in \mathrm{AB},\ \mathrm{BG},\ \mathrm{HC},\ \mathrm{CD},\ \mathrm{DF},\ \mathrm{EA}, \end{cases} \tag{77}$$

where $\boldsymbol{n}$ is the outward normal of the rectangle region, and V_g is the gate voltage. Here, electron penetration into the oxide regions is neglected, so transport equation is considered only in the silicon layer, and the gate voltage V_g is imposed on gates EF and GH. The floating boundary condition, i.e. a homogeneous Neumann condition, maintains macroscopic space charge neutrality at the source (drain) end despite of the biasing condition. The rectangle region is taken as the computational domain for the Green's function.

The bias voltage is set as $V_{ds} = 0.4$ eV. We analyze the numerical convergence order of FDM and FEM, by taking the numerical result with $a = 0.15, b = 0.05$ as the reference solution. Table 1 gives the numerical converge order of the two methods by comparing the results with $a = 0.9, b = 0.2$ and the results with $a = 0.45, b = 0.1$. We obtain a second-order convergence.

Fig. 12 is the potential distribution under the gate bias $V_g = 0.4$ eV and drain bias $V_{ds} = 0.4$ eV, and Fig. 13 is the density distribution. Fig. 14 is the potential distribution at the center of the silicon layer with the two numerical methods. To compare the precision of the two numerical methods, we also plot the absolute error

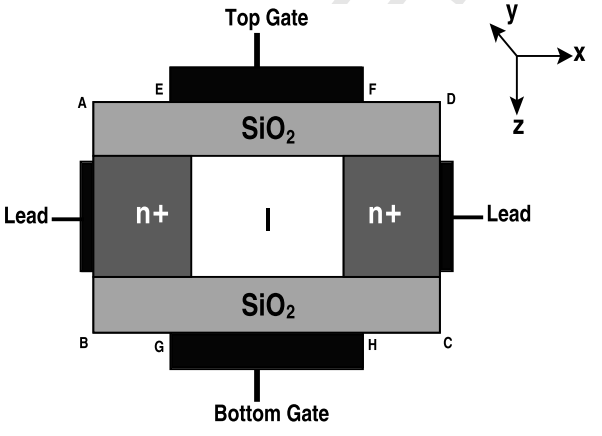

Fig. 11. A ultra-thin double gate MOSFET structure. The computational region is the rectangle ABCD.

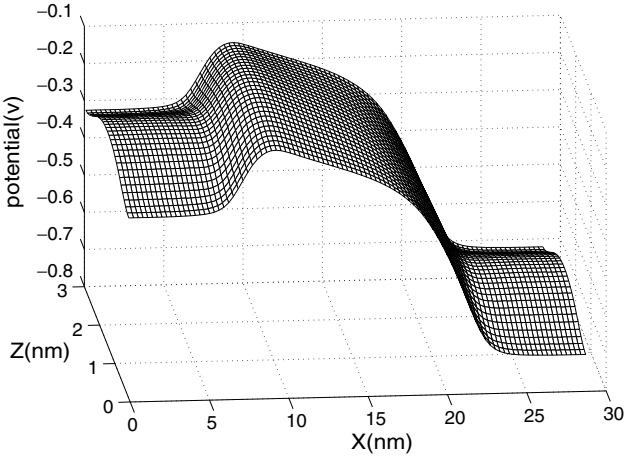

Fig. 12. Double gate MOSFET: the potential distribution in the silicon layer. $V_g = 0.4$ eV, $V_{ds} = 0.4$ eV.

Please cite this article in press as: H. Jiang et al., Boundary treatments in non-equilibrium Green's ..., J. Comput. Phys. (2008), doi:10.1016/j.jcp.2008.03.018

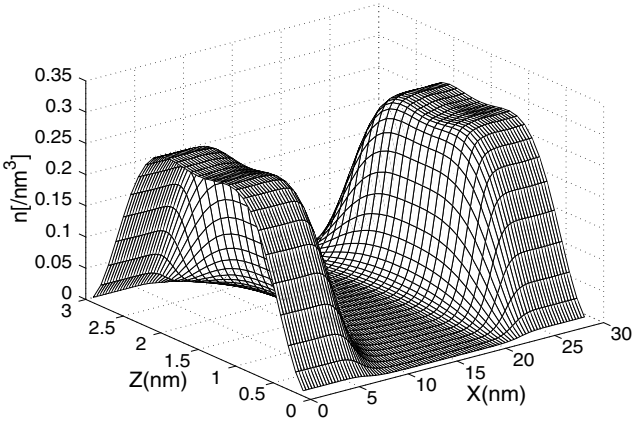

Fig. 13. Double gate MOSFET: the density distribution in the silicon layer. $V_g = 0.4$ eV,$V_{ds} = 0.4$ eV.

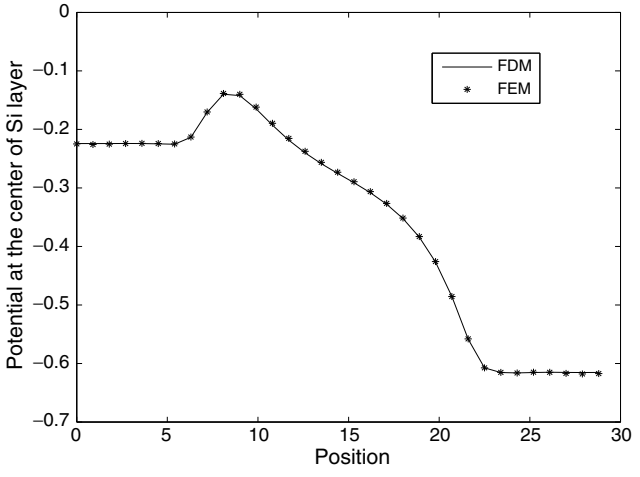

Fig. 14. Double gate MOSFET: the potential at the center of the silicon layer with FDM and FEM.

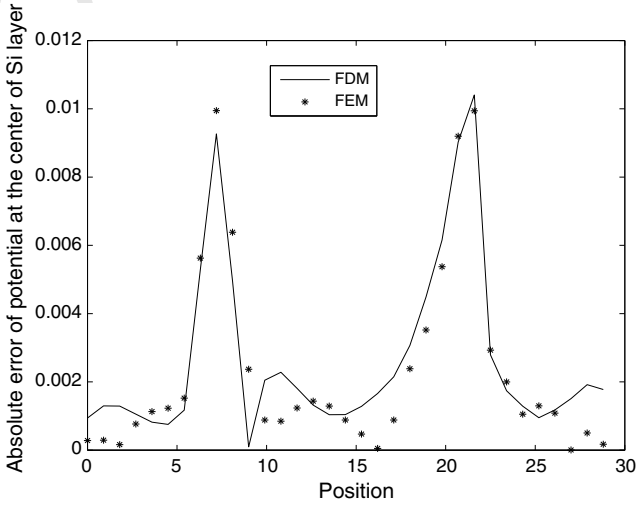

Fig. 15. Double gate MOSFET: the absolute error of the potential at the center of the silicon layer with FDM and FEM.

Please cite this article in press as: H. Jiang et al., Boundary treatments in non-equilibrium Green's ..., J. Comput. Phys. (2008), doi:10.1016/j.jcp.2008.03.018

of the potential at the center of the silicon layer in Fig. 15. Numerical results show that FEM performs better than FDM for the double gate MOSFET simulation.

5. Conclusions

In this paper, we provide a unified treatment of the quantum device boundaries in the formalism of non-equilibrium Green's functions for quantum transport under biased external potentials. The boundary treatments, namely, the device boundary self-energies Σ representing the influence of the quantum device geometry on the transport, are obtained by using exterior auxiliary Green's functions. Second-order FDM and FEM discretizations of the NEGF are solved with a Poisson equation in a self-consistent iteration. Numerical results demonstrated the accuracy and flexibility of the proposed boundary treatment of the quantum devices. An improved computation for spectral function is applied to simulate a 29 nm double gate MOSFET.

Acknowledgments

The authors are grateful to Prof. Xiaoyang Liu for helpful discussions. S.H. Shao is partially supported by China Scholarship Council (CSC). W. Cai thanks the support of Army Research Office (Grant No.: W911NF-07-1-0492). P.W. Zhang is partially supported by National Science Foundation of China for Distinguished Young Scholars 10225103 and 90207009.

Appendix. Green's function in contacts

The analytical expressions of $g(\boldsymbol{r},\boldsymbol{r}')$ used in this paper are listed below. The interested readers can find some similar derivations in [2,23] for more details.

One-dimensional contact

The retard Green's function in the infinite one-dimensional wire satisfies

$$\left(E - v^{\alpha} + \frac{\hbar^2}{2m^{\alpha}}\frac{\partial^2}{\partial x^2}\right)\tilde{g}(x,x') = \delta(x-x'), \tag{A.1}$$

the solution of which reads

$$\tilde{g}(x,x') = \frac{m^{\alpha}}{\mathrm{i}k^{\alpha}\hbar^2}\exp(\mathrm{i}k^{\alpha}|x-x'|), \tag{A.2}$$

where v^{α} is a constant potential and $k^{\alpha} = \sqrt{\frac{2m^{\alpha}(E-v^{\alpha})}{\hbar^2}}$. Then, the Green's function defined in semi-infinite one-dimensional wire with the end $x = d$ is

(1) if $g(d,x') = 0$, then

$$g(x,x') = \tilde{g}(x,x') - \tilde{g}(2d-x,x'); \tag{A.3}$$

(2) if $\frac{\partial g(d,x')}{\partial x} = 0$, then

$$g(x,x') = \tilde{g}(x,x') + \tilde{g}(2d-x,x'). \tag{A.4}$$

Two-dimensional semi-infinite strip-shaped contact

The retard Green's function in an infinite strip wire satisfies

$$\left(E - v^{\alpha}(z) + \frac{\hbar^2}{2m^{\alpha}}\nabla^2\right)\tilde{g}(\boldsymbol{r},\boldsymbol{r}') = \delta(\boldsymbol{r}-\boldsymbol{r}'), \tag{A.5}$$

the solution of which reads, for $\boldsymbol{r} = (x,z)$ and $\boldsymbol{r}' = (x',z')$

$$\tilde{g}(\boldsymbol{r},\boldsymbol{r}') = \sum_l \frac{m^{\alpha}}{\mathrm{i}k_l^{\alpha}\hbar^2}\chi_l^{\alpha}(z)\chi_l^{\alpha}(z')\exp(\mathrm{i}k_l^{\alpha}|x-x'|), \tag{A.6}$$

where $\chi_l^\alpha(z)$ satisfies

$$\left(-\frac{\hbar^2}{2m^\alpha}\frac{\partial^2}{\partial z^2}+v^\alpha(z)\right)\chi_l^\alpha(z)=\lambda_l^\alpha\chi_l^\alpha(z), \tag{A.7}$$

and $k_l^\alpha=\sqrt{\frac{2m^\alpha(E-\lambda_l^\alpha)}{\hbar^2}}$. It is noted that the normalized eigenfunctions are used here. Then, the Green's function in a semi-infinite strip wire with a straight line boundary $x=d$ is

(1) if $g(d,z,\mathbf{r}')=0$, then

$$g(\mathbf{r},\mathbf{r}')=\tilde{g}(x,z,\mathbf{r}')-\tilde{g}(2d-x,z,\mathbf{r}'); \tag{A.8}$$

(2) if $\frac{\partial g(d,z,\mathbf{r}')}{\partial x}=0$, then

$$g(\mathbf{r},\mathbf{r}')=\tilde{g}(x,z,\mathbf{r}')+\tilde{g}(2d-x,z,\mathbf{r}'). \tag{A.9}$$

Two-dimensional semi-infinite wedge-shaped contact

The semi-infinite contact wedge-shaped area is shown in Fig. 16. The whole wedge is denoted by $\widetilde{\Omega}_\alpha=\{(r,\theta)|0<r<+\infty,0<\theta<\beta\}$. The retard Green's function in the infinite wedge area $\widetilde{\Omega}_\alpha$ satisfies

$$\left(E-v^\alpha+\frac{\hbar^2}{2m^\alpha}\left(\frac{1}{r}\frac{\partial}{\partial r}\left(r\frac{\partial}{\partial r}\right)+\frac{1}{r^2}\frac{\partial^2}{\partial\theta^2}\right)\right)\tilde{g}(r,\theta,r',\theta')=\delta(r-r')\delta(\theta-\theta'), \tag{A.10}$$

with a homogeneous Dirichlet boundary condition on $\partial\widetilde{\Omega}_\alpha$, the solution of which can be obtained by an image approach proposed in [24]. Then, the Green's function defined in the semi-infinite wedge contact Ω_α is given as

$$g(r,\theta,r',\theta')=\tilde{g}(r,\theta,r',\theta')-\widetilde{h}(r,\theta), \tag{A.11}$$

where $\widetilde{h}(r,\theta)$ satisfies the same Eq. (A.10) but with zero RHS term and a homogeneous Dirichlet condition on $\Gamma_{\alpha,0}$. And,

$$\widetilde{h}(r,\theta)=\tilde{g}(r,\theta,r',\theta'),\quad (r,\theta)\in\Gamma_\alpha, \tag{A.12}$$

for $g(r,\theta,r',\theta')$ satisfying homogeneous Dirichlet condition on Γ_α, or

$$\frac{\partial\widetilde{h}(r,\theta)}{\partial r}=\frac{\partial\tilde{g}(r,\theta,r',\theta')}{\partial r},\quad (r,\theta)\in\Gamma_\alpha, \tag{A.13}$$

for $g(r,\theta,r',\theta')$ satisfying homogeneous Neumann condition on Γ_α. The general solution of $\widetilde{h}(r,\theta)$ is in the form of

$$\widetilde{h}(r,\theta)=\sum_l c_l F_l(k^\alpha r)\sin\frac{l\theta\pi}{\beta}, \tag{A.14}$$

where c_l are undetermined coefficients,

$$k^\alpha=\sqrt{\frac{2m^\alpha|E-v^\alpha|}{\hbar^2}},\quad\text{and}\quad F_l(x)=\begin{cases}H_l^{(2)}(x) & E\geqslant v^\alpha\\ K_l(x) & \text{otherwise}\end{cases} \tag{A.15}$$

with the Hankel function of the second kind $H_l^{(2)}(x)$ and the modified Bessel function of the second kind $K_l(x)$. For the small contact area in most applications, Γ_α can be assumed (or approximated) as an arc $r(\theta)=r_0$, and using Eqs. (A.12) and (A.13), we have

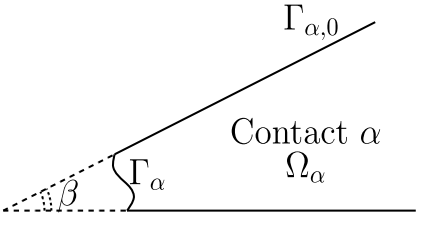

Fig. 16. Semi-infinite wedge-shaped contact in the polar coordinates (r,θ). $\Gamma_\alpha=\{(r,\theta)|r=r(\theta),0\leqslant\theta\leqslant\beta\}$, $\Omega_\alpha=\{(r,\theta)|r(\theta)<r<+\infty,0<\theta<\beta\}$, and $\Gamma_{\alpha,0}=\{(r,\theta)|r(0)\leqslant r<+\infty,\theta=0;r(\beta)\leqslant r<+\infty,\theta=\beta\}$.

Please cite this article in press as: H. Jiang et al., Boundary treatments in non-equilibrium Green's ..., J. Comput. Phys. (2008), doi:10.1016/j.jcp.2008.03.018

(1) if $g(r_0, \theta, r', \theta') = 0$, then

$$c_l = \frac{2}{\beta F_l(k^\alpha r_0)} \int_0^\beta \widetilde{g}(r_0, \theta, r', \theta') \sin \frac{l\theta\pi}{\beta} \mathrm{d}\theta; \tag{A.16}$$

(2) if $\frac{\partial g(r_0,\theta,r',\theta')}{\partial r} = 0$, then

$$c_l = \frac{2}{\beta k^\alpha (F_l(k^\alpha r_0))'} \int_0^\beta \frac{\partial \widetilde{g}(r_0, \theta, r', \theta')}{\partial r} \sin \frac{l\theta\pi}{\beta} \mathrm{d}\theta. \tag{A.17}$$

If Γ_α is a general curve shown in Fig. 16, a numerical approximation by a collocation method along Γ_α may be used to find approximations for c_l.

References

[1] D. Ferry, S.M. Goodnick, Transport in Nanostructures, Cambridge University Press, Cambridge, 1997.
[2] S. Datta, Electronic Transport in Mesoscopic Systems, Cambridge University Press, Cambridge, 1995.
[3] H. Haug, A.P. Jauho, Quantum Kinetics in Transport and Optics of Semi-conductors, second ed., Springer, 2007.
[4] S. Datta, Nanoscale device modeling: the Green's function method, Supperlattices Microstruct. 28 (2000) 253–278.
[5] R. Venugopal, M. Paulsson, S. Goasguen, S. Datta, M.S. Lundstrom, A simple quantum mechanical treatment of scattering in nanoscale transistors, J. Appl. Phys. 93 (2003) 5613–5625.
[6] Z. Ren, R. Venugopal, S. Goasguen, S. Datta, M.S. Lundstrom, NanoMOS 2.5: a two-dimensional simulator for quantum transport in double-gate MOSFETs, IEEE Trans. Electron Devices 50 (2003) 1914–1925.
[7] R. Venugopal, Z. Ren, S. Datta, M.S. Lundstrom, D. Jovanovic, Simulating quantum transport in nanoscale transistors: real versus mode-space approaches, J. Appl. Phys. 92 (2002) 3730–3739.
[8] P. Havu, V. Havu, M.J. Puska, R.M. Nieminen, Nonequilibrium electron transport in two-dimensional nanostructures modeled using Green's functions and the finite-element method, Phys. Rev. B 69 (2004) 115325.
[9] E. Polizzi, S. Datta, Multidimensional nanoscale device modeling: the finite element method applied to the non-equilibrium Green's function formalism, in: Proceedings of the 2003 Third IEEE Conference on Nanotechnology, pp. 40–43.
[10] J. Wang, E. Polizzi, M. Lundstrom, A three-dimensional quantum simulation of silicon nanowire transistors with the effective-mass approximation, J. Appl. Phys. 96 (2004) 2192–2203.
[11] H.D. Han, X.N. Wu, Approximation of infinite boundary condition and its application to finite element methods, J. Comput. Math. 3 (1985) 179–192.
[12] D. Givoli, Non-reflecting boundary conditions, J. Comput. Phys. 94 (1991) 1–29.
[13] V.A. Baskakov, A.V. Popov, Implementation of transparent boundaries for numerical solution of the Schrödinger equation, Wave Motion 14 (1991) 123–128.
[14] J.R. Hellums, W.R. Frensley, Non-Markovian open-system boundary conditions for the time-dependent Schrödinger equation, Phys. Rev. B 49 (1994) 2904–2906.
[15] F. Schmidt, P. Deuflhard, Discrete transparent boundary conditions for the numerical solution of Fresnel's equation, Comput. Math. Appl. 29 (1995) 53–76.
[16] J.S. Papadakis, Impedance formulation of the bottom boundary condition for the parabolic equation model in the underwater acoustics, NORDA Parabolic Equation Workshop, NORDA Tech. Note 143, 1982.
[17] A. Arnold, M. Ehrhardt, Discrete transparent boundary conditions for wide angle parabolic equations in underwater acoustics, J. Comput. Phys. 145 (1998) 611–638.
[18] A. Arnold, M. Ehrhardt, I. Sofronov, Discrete transparent boundary conditions for the Schrödinger equation: fast calculation approximation and stability, Commun. Math. Sci. 1 (2003) 501–556.
[19] S. Jiang, L. Greengard, Fast evaluation of nonreflecting boundary conditions for the Schrödinger equation in one dimension, Comput. Math. Appl. 47 (2004) 955–966.
[20] C.S. Lent, D.J. Krikner, The quantum transmitting boundary method, J. Appl. Phys. 67 (1990) 6353–6359.
[21] E. Polizzi, N.B. Abdallah, Subband decomposition approach for the simulation of quantum electron transport in nanostructures, J. Comput. Phys. 202 (2005) 150–180.
[22] C. Cheng, J.H. Lee, K.H. Lim, H.Z. Massoud, Q.H. Liu, 3D quantum transport solver based on the perfectly matched layer and spectral element methods for the simulation of semiconductor nanodevices, J. Comput. Phys. 227 (2007) 455–471.
[23] S.H. Shao, W. Cai, H.Z. Tang, Accurate calculation of Green's function of the Schrödinger equation in a block layered potential, J. Comput. Phys. 219 (2006) 733–748.
[24] M.E. Ermutlu, I.V. Lindell, K.I. Nikoskinen, Two-dimensional image theory for the conducting wedge, J. Electromagn. Waves Appl. 7 (1993) 971–986.

Please cite this article in press as: H. Jiang et al., Boundary treatments in non-equilibrium Green's ..., J. Comput. Phys. (2008), doi:10.1016/j.jcp.2008.03.018